*Original Article*

High Performance Polymers

High Performance Polymers
2023, Vol. 35(9) 936–945

DOI: 10.1177/09540083231191416
journals.sagepub.com/home/hip



# Structure and properties of thermoplastic polyimide based on 4′,4′—(oxybis (methylene)) bis ([1.1′- bipheny]3-amine) diamine

**Jinshui Lu[1], Jinyuan Zhang[1], Heng Liu[1], Weipeng Chen[1], Jiangrong Luo[1], Ziqing Wang[1], Tingting Cui[1], Yonggang Min[1] and Yidong Liu[2]**

## Abstract

In this work, a new diamine was designed by connecting flexible structures such as ether bond and aliphatic carbon chain between benzene rings, and was synthesized and purified through simple reactions such as Suzuki reaction. Finally, a series of polyimide (PI) films were synthesized by copolymerization with 4.4`-diaminodiphenyl ether (ODA)\pyromellitic dianhydride (PMDA) in different proportions. We prepared polyimide films with new monomer copolymerization ratios of 1% (PI-1), 5% (PI-2), 10% (PI-3), and 20% (PI-4). The polyimide films showed excellent glass transition temperatures, which were attributed to their unique bent architectures. The mechanical and thermal properties of the thermosets were studied using tensile testing, static thermomechanical analysis (TMA), and thermogravimetric analysis (TGA). As the results, the films exhibited the optimal glass transition temperatures (317.56°C–381.91°C), and the component with the highest copolymerization ratio has a 15% decrease in glass transition temperature compared to the component without copolymerization. Moreover, PI-1-PI-4 showed good heat resistance in the N2 atmosphere. The temperatures corresponding to a 5% heat loss in the films (T5%) were 458.12 °C–548.75°C, respectively.

## Keywords

Polyimide, glass transition temperatures, films, thermal properties

## Introduction

Polyimide is a kind of engineering polymer with high-temperature resistance, belonging to the class of high-performance plastics. Polyimide is produced from the polyamide acid (PAA) solution formed by dehydration and condensation of diamine and dianhydride in N,N-dimethylacetamide (DMAC), N-methylpyrrolidone (NMP), and other polar solvents. The solution is then exposed to solvent removal, high-temperature imidization or chemical imidization to obtain the final product. Possessing a rigid structure, the traditional polyimide is basically thermosetting because of the high glass transition temperature (close to 400°C), which makes its further processing more complicated. Meanwhile, if polyimides could be reprocessed like polypropylene (PP) and polyethylene (PE), their range of use would be greatly enlarged.[1–5]

At a glance, there is a variety of polyimides, especially in the high-tech field. This is due to the fact that ordinary plastics and polymers often fail to meet rigorous requirements for high-temperature resistance applications like aerospace vehicles, electronic devices, and medical instruments.[6–16] For example, the components for many electronic industries a (e.g., lead-free reflow soldering) must withstand the temperature of 270°C for a long time or be able to process at 400°C for a short time. In that regard, high-performance polyimides allow one to address the above issues. However, regardless of high-temperature resistance, polyimides have disadvantages associated with

[1]School of Materials and Energy, Guangdong University of Technology, Guangzhou, China
[2]Institute of Mechanics, Chinese Academy of Sciences, Beijing, China

**Corresponding authors:**
Yonggang Min, School of Materials and Energy, Guangdong University of Technology, Guangzhou 510006, China.
Email: ygmin@gdut.edu.cn

Yidong Liu, Institute of Mechanics, Chinese Acedemy of Sciences, Beijing 100190, China.
Email: liuyd@imech.ac.cn

structural rigidity owing to the presence of numerous aromatic benzene rings, which make polyimide processing laborious. To solve this problem, many studies have been dedicated to the design and synthesis of diamine or dianhydride with flexible groups, such as ether bonds, aliphatic linkages, and carbonyl groups, or the introduction of asymmetric non-coplanar structures.[17–25] Nevertheless, abundant flexible components may affect the heat resistance of polyimide.

Therefore, there should be a balance between the low enough glass transition temperature and processing flexibility without sacrificing heat resistance. Recently, the copolymerization of rigid diamine and flexible diamine has been proposed as a reliable way to maintain heat resistance of processable polyimides at a high level.[26]

So far, the manufacturing of thermoplastic polyimides has been a challenge for the following reason. Copolymerization with common pyromellitic dianhydride (PMDA), biphenyl tetraic anhydride (BPDA), and other types of dianhydrides in a ratio of 1:1 entail excessive consumption of monomers, such as diamine, which is hard to achieve on an industrial scale. Therefore, the present study was aimed at developing the simplest and most labor-saving synthesis method to obtain diamine so as to satisfy user's needs. Specifically, a new kind of diamine was produced through a two-step Suzuki reaction. Diamine had not only flexible parts, such as ether bonds and fatty chains but also the aromatic coarse rigid structure, which was conducive to the increase in its applicability range. Besides that, attention was paid to the mechanical and thermal properties of the polyimide synthesized through the copolymerization of diamine so as to distinguish the solution with the lowest copolymerization ratio. According to the findings, the improvement in the characteristics of traditional polyimide films obtained via copolymerization, along with reduced time and costs, is promising for their future large-scale production.

## Experiments

### Materials

The intermediate 2-1 was prepared by using p-bromobenzaldehyde (97%, Aladdin), trifluoromethylsulfonic acid (Aladdin), triethylsilane (Mackling), dichloromethane (Mackling) and other raw materials. (3-aminophenyl) boric acid (97%, Macklin), ethanol (99%, Macklin), sodium carbonate (99%, Mcklin), tetra (triphenylphosphine) palladium (99%, J&K Scientific), used for Suzuki reaction to prepare new diamine 3-1. N, N-dimethylformamide (Macklin), toluene (Aladdin), petroleum ether (Mackln), dichloromethane (Macklin), ethyl acetate (Aladding), deionized water, etc. Are used as solvent or mobile phase for column chromatography.

### Characterization

Gel permeation chromatography (GPC): measured by U3000 high performance liquid chromatograph from Thermo Fish, Shanghai, China.

Dynamic viscosity test: use the NDJ-1S digital viscometer of Hengping Company in Shanghai, China for testing.

Liquid mass spectrometry: TSQ Endura ultra-high performance liquid chromatography tandem triple quadrupole mass spectrometer of Thermo Fisher Scientific Co., Ltd in Shanghai, China was used for determination.

Nuclear magnetic resonance ($^1$H-NMR) test: use V ANCEIIIHD400 NMR instrument from Bruker, Switzerland for determination.

Infrared spectrum (FT-IR) test: use Nicolet ATR-60 Fourier transfor m infrared spectrometer from Thermo Fish in Shanghai, China for scanning.

Thermogravimetric analysis (TGA): TGA/DSC 3+thermogravimetric analyzer from Mettler Toledo, Zurich, Switzerland is used for testing. In a nitrogen atmosphere of 10°C/min, raise the temperature to 800°C at a flow rate of 50 mL/min.

XRD test: Bruker D8ADV ANCE X-ray diffractometer, copper target, tube voltage 40 kV, tube current 40 mA,s-canning angle 2θRange 6° to 60°, scanning speed 6°/min

Mechanical property testing: The AG-X plus electronic universal material testing machine from Shimadzu, Japan was used for testing. The sample size was a rectangular film strip of 1 × 5 cm, the stretching rate was 50 mm/min, and the test was repeated five times.

Thermomechanical analysis (TMA): The test was performed with a TMA-Q400EM thermomechanical analyzer from TA Instruments, New Castle, USA, with a rectangularsample strip of 5 mm width and a constant tensile force of 50 mN.

Contact angle: Using SL200KB contact angle tester from KINO Industrial, Boston,MA, USA.

### Computer simulation

In order to investigate the effect of copolymerization ratio on the glass transition temperature of 4′, 4′ - (oxybis (methylene)) bis (([1.1′- biphenyl] - 3-amine)) (OBBA)/ODA/PMDA systems, we calculated their Fractional Free Volume (FFV), and roughly simulated their glass transition temperature based on the change of specific volume/density with temperature. In addition, in order to obtain a better modeling structure, we conducted five cycles of temperature and temperature cycling annealing under isothermal isovolumetric thermodynamic conditions (NVT) in the range of 300-700-300 K. Existing relevant researchers have determined through simulation calculations that molecular chains with a polymerization degree of 10–15 can basically

meet the calculation accuracy requirements, but those with a copolymerization ratio of 1% cannot be simulated. Therefore, in this paper, the polymerization degree of polymer molecular chains is set to 100. The model is based on 100 units of monomers, in which copolymerization ratios of 1%, 5%, 10%, and 20% are calculated and simulated.

The model starts at 300 K and heats up once every 25 K until it reaches 700 K. The whole process goes through 17 stages. After 700 K, the above model is still followed for cooling treatment, and the temperature is lowered every 25 K. The stage cooling curve is taken for subsequent analysis. Through molecular dynamics simulation of the NVT system, the simulated polyimide system has a temperature fluctuation difference of less than 10% and an energy fluctuation range of no more than 3% within a fixed time of 500 ps at 300 K. This proves that the structure is completely relaxed and in equilibrium.

## Synthesis and characterization of polyimide film

### *Synthesis of 4.4′- (oxybis (methylene)) bis (bromobenzene)*

First, p-bromobenzaldehyde (30 g, 0.172 mol), triethylsilane (30 mL, 0.189 mol), and trifluoromethylsulfonic acid (1.9662 g, 13 mmol) were put into a conical flask containing 100 mL of dichloromethane solvent. The flask was then placed on the magnetic heating table for stirring at room temperature for 24 h. Deionized water and excessive dichloromethane were afterward added to the mixture to extract the organic layer and reduce the solution. After that, the blend was dried and filtered with anhydrous magnesium sulfate (MgSO4). The redundant solvent was then eliminated under negative pressure on the rotary evaporator, and the crude product was purified via column chromatography (silica gel, petroleum ether/ethyl acetate). White products were finally obtained after freeze drying. Yield: 18 g (63%). As shown in Figure 1 and Scheme 1. $^{1}$H NMR (400 MHz, Chloroform-d) δ 7.55 – 7.47 (m, $^{1}$H), 7.27 (d, J = 8.4 Hz, $^{1}$H), 4.68 (s, $^{1}$H).

### *Synthesis of 4′, 4′ - (oxybis (methylene)) bis (([1.1′- biphenyl]—3-amine)) (biphenyl OBBA)*

The previously obtained compound (10 g, 2.8 mmol) was diluted in 100 mL of toluene. Then, 3-aminophenyl boric acid (9.24 g, 6.7 mmol), ethanol (67.41 mL, 13.4 mmol), and sodium carbonate solution (67.41 mL, 13.4 mmol) were added to the solution under stirring until their complete dissolution. After nitrogen bubbling for 20 min, a Pd catalyst ($PPh_3)_4$ (0.78 g, 0.67 mmol) was introduced into the system, and the reaction therein was then initiated by heating to 70°C for 24 h. The organic layer was thus extracted, the solvent was further evaporated by drying on a rotary evaporator, and 4′, 4′ - (oxybis (methylene))) bis (([1.1′- biphenyl] - 3-amine) (OBBA) was produced via separation and purification using column chromatography (ethyl acetate/dichloromethane/petroleum ether). As shown in Figure 2 and Scheme 2. $^{1}$H NMR (400 MHz, Chloroform-d) δ 7.59 – 7.52 (m, $^{1}$H), 7.46 – 7.39 (m, $^{1}$H), 7.21 (d, J=7.8 Hz, $^{1}$H), 7.02 – 6.96 (m, $^{1}$H), 6.90 (t, J=2.0 Hz, $^{1}$H), 6.71 – 6.63 (m, $^{1}$H), 4.62 (s, $^{1}$H), 3.73 (s, $^{1}$H). m/z: (m+H)+calculation. 380.49 for $C_{26}H_{24}N_2O$. Found, 381.17.

### *Preparation of PI membrane (PI-a)*

DMAC (17.347)、OBBA and ODA (0.01 mol in total) were poured into a flask with a mixing device under low-humidity conditions (about 15%) at room temperature. Then, PMDA (2.2042 g, 0.01 mol) were added to the system with a small spoon after the diamine complete dissolution so that the viscosity of the solution increased to a large extent. After continuous mixing for 6 h, bubbles were removed under reduced pressure, and the polyamide acid slurry was evenly applied onto the round glass substrate with a glue homogenizer. The material was afterward heated in an oven at 80°C–90°C for 25-35 min to eliminate excessive solvent and a small amount of water inside. The polyimide film was then obtained by thermal imidization at the programmed temperature (250°C–350°C) and peeled off of the substrate using ultrasound. A series of polyimide films with different biphenyl OBBA contents (0%, 1%, 5%, 10%, and 20%) were prepared by repeating the above steps. According to the copolymerization ratio, films were labeled as PI-0, PI-1, PI-2, PI-3, and PI-4, respectively. As shown in Scheme 3, we can see the specific chemical process of the above process. As shown in 3.e can see the specific chemical process of the above process.

## Results and discussions

### *Polyamide acid performance analysis*

The relative molecular weight and dynamic viscosity of polyamide acid (PAA) were assessed by means of gel permeation chromatography (GPC) and viscometry, respectively. As seen from Table 1, with the increase of the molecular weight of OBBA monomer, that of PAA glue showed an upward trend, whereas the dynamic viscosity first increased and then decreased. The introduction of diamine monomers containing ether bonds and aliphatic linkages made the polyamide molecular chains more flexible, which simplified their contact with the newly added dianhydride during the synthesis process. As a result, the polyamide molecular chain length and polyamide molecular weight were substantially increased. Moreover, there were

**Table 1.** Relative molecular weight and dynamic viscosity of monomer PAA with different molar concentrations.

| Name/Scale | PI-0 | PI-1 | PI-2 | PI-3 | PI-4 |
|---|---|---|---|---|---|
| Mn | 394339 | 553804 | 262852 | 581901 | 334828 |
| Mw | 394348 | 558425 | 262868 | 583931 | 414141 |
| Mz | 394357 | 562755 | 262883 | 585829 | 476382 |
| PPD | 1.00 | 1.01 | 1.00 | 1.00 | 1.24 |
| Viscosity (mPa·s) | 8090 | 3228 | 15752 | 22991 | 5904 |

noticeable changes in viscosity with varying copolymerization ratio. At the low OBBA content, the viscosity remained at a high level due to a small amount of flexible chains in the PAA glue that quite easily penetrated the relatively rigid part of the structure. This led to the formation of clusters and entanglements, manifesting themselves by the increase of viscosity on the macro level. However, at a certain degree of copolymerization, the flexibility of each segment within the molecular chain was greatly improved, preventing clustering and entanglement as easily as before and thus reducing the viscosity of the polymer on the macro level. Figure 1 and 2.

## *Fourier transform infrared spectroscopy analysis*

The chemical structures of PI films were characterized via Fourier transform infrared (FT-IR) spectroscopy, and the corresponding spectra are shown in Figure 3. The five groups of PI films after thermal imidization exhibited well-resolved characteristic absorption peaks at 1778, 1720, 1370, and 722 $cm^{-1}$. Those at 1778 $cm^{-1}$ were ascribed to the imide C=O asymmetric to tensile vibrations; the features at 1720 $cm^{-1}$ took their origin from the C=O asymmetric to tensile vibrations of the imide ring; the peaks at 1370 $cm^{-1}$ were attributed to the tensile vibration of C-N imide rings, and the band at 722 $cm^{-1}$ was associated with the C=O bending vibration. It is noteworthy that no other peaks related to carboxyl (-COOH), amide (-CO-NH-), or residual amino (-NH-) groups in the range of 3300–3500 $cm^{-1}$ were detected, indicating that polyimide was completely amidated.

## *XRD results*

In order to explore the aggregation mechanism, such as the spacing between the molecular chains in the polyimide films, the specimens were examined via XRD. As shown in Figure 4, with the increase of the copolymerization ratio, the XRD peak of flexible diamine changed from flat to sharp and then to flat, meaning that the polyimide film was not crystallized. In addition, the peak shifted from 19° to 20°. The relationship between the diffraction angle and the interchain spacing is expressed by the Bragg equation $2d\sin\theta = n\lambda$, where d is the inteplanar spacing in the crystal cell. The larger the d value, the

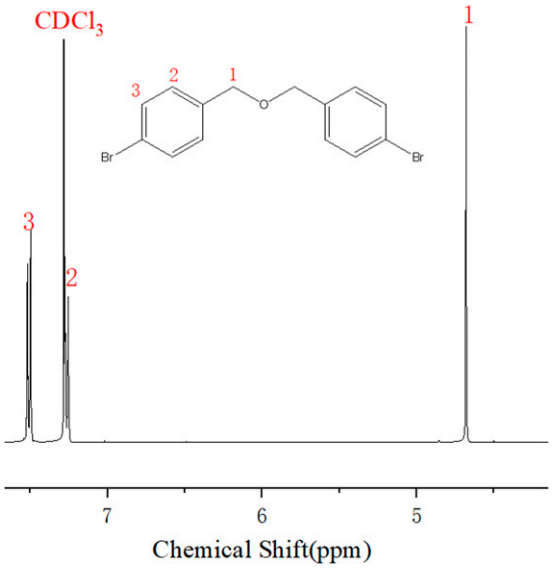


**Figure 1.** 1H NMR spectra of intermediates.

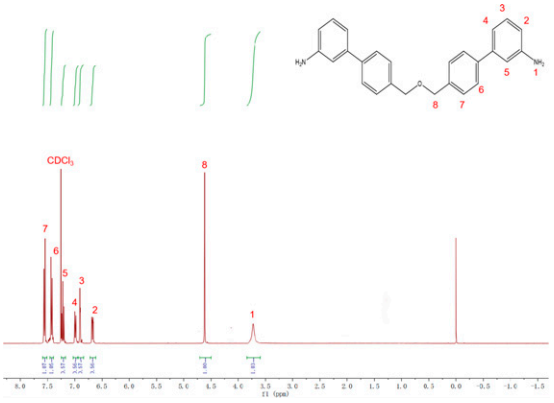


**Figure 2.** 1H NMR spectrum of NADA.

larger the interchain distance and free volume, and vice versa. Table 2 displays the calculated parameters. According to the table, the interchain spacing decreased with the increase of the copolymerization ratio, which was due to numerous flexible ether bonds and fatty chains in the newly produced diamine monomer. The enhancement in flexibility caused the stacking of chains, thereby reducing the spacing between them. Regardless of lots of biphenyl moieties in the diamine structure,

the contribution from flexible components to the flexibility of the whole system was greater than that from the rigid biphenyl. Moreover, a symmetric structure was conducive to the orderly arrangement and stacking of chains in diamine, thus reducing its free volume and making the molecular chains denser.

## *Thermal properties and thermal expansion coefficient of polyimide film*

The thermal stability of polymer films was studied via the thermogravimetric analysis (TGA), and the corresponding TGA curves are shown in Figure 5. As seen in Table 3, the thermal performance of the copolymerized films was superior to that before copolymerization. At the 5% weight loss of the copolyimide, the thermal decomposition temperature of PI0-PI4 specimens was in the range of 458°C–548°C. At the 10% weight loss, the thermal decomposition temperature varied between 532 and 572°C. At 800°C, the carbon residue rate in the polyimide films was 49.69%–56.41%. At the copolymerization ratio of 1%–10%, the thermal decomposition temperature (Td5%), the thermal decomposition temperature (Td10%), and the decomposition temperatur (RW800°) values significantly increased, among which Td5% changed to the greatest extent. Moreover, the number of flexible chain segments increased with the increase in the proportion of flexible diamine, which enhanced the stacking and entanglement with rigid chain segments. In addition, the amount of benzene rings in the copolymerized diamine was also larger than that of ODA. At the low copolymerization ratio, benzene rings contribution to the thermal properties of the polymer exceeded that of the flexible chain segments, which considerably improved the heat resistance of the material. However, once the copolymerization ratio rose to a certain extent, the impact of the flexible chain segments on the thermal properties was far stronger than that of the rigid chain segments, thus reducing the thermal decomposition temperature to some level but not less than 450°C.

Many studies have shown that the thermal expansion coefficient is closely related to the glass transition temperature of polymers.[27] When the temperature is below the glass transition point, the polymer chain segment is frozen, and its internal thermal expansion factor is mainly determined by the van der Waals force between the molecular

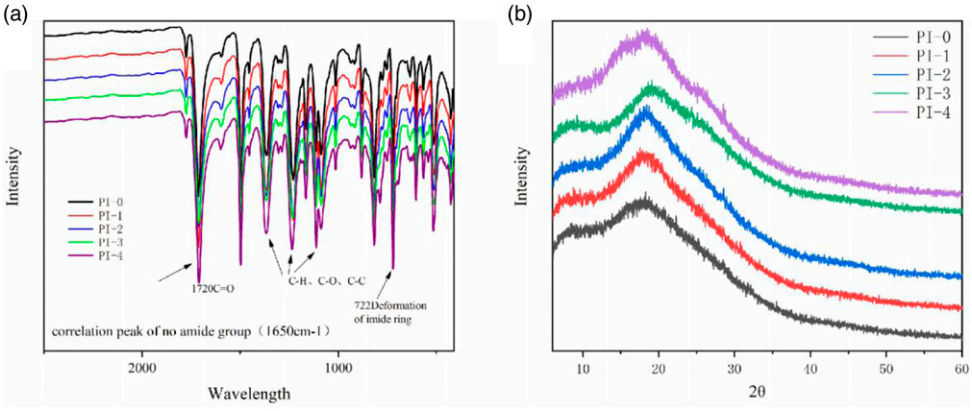


**Figure 3.** (a) FTIR spectra of the PI films (b) XRD of polyimide film.

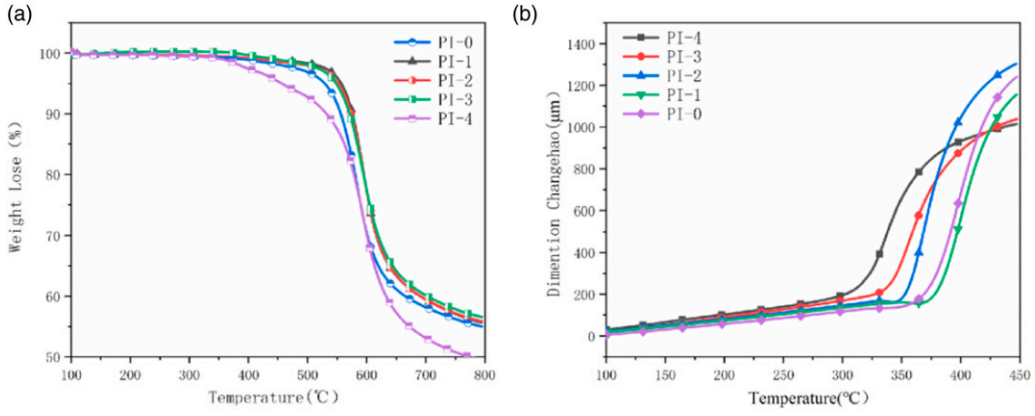


**Figure 4.** (a) TGA curve of polyimide film (b) TMA curve of polyimide filmig.

chains and the intramolecular force. At this stage, the difference between the thermal expansion coefficients of polyimides with different copolymerization ratios remains small. Once the temperature reaches the glass transition point of the polymer, the segments are completely thawed, allowing the molecular chain to move freely. At the same time, thermal movement will also occur due to heating. The free volume between the flexible chains becomes larger, and the fluidity gets stronger, thereby increasing the thermal expansion coefficient of the polymer with abundant, flexible molecular chains. Figure 6 displays the size-temperature plots, in which the slopes before and after the intersection (Tg) point (550K-650K) were taken to calculate the CTEs of the films. According to Table 3, with the increase of the copolymerization ratio, the glass transition temperature of the PI film dramatically decreased from 374°C to 317°C, which was owing to the presence of flexible structures, such as ether bonds and fatty chains. The chain segments within the molecule were able to freely bend and twist, providing plenty of single bonds for rotation. As a result, the flexibility of the polymer was greatly improved, and its glass transition temperature was drastically reduced Figure 7.

**Table 2.** Diffraction peak and chain spacing of PI film.

| | PI-0 | PI-1 | PI-2 | PI-3 | PI-4 |
|---|---|---|---|---|---|
| 2θ(°) | 18.958 | 19.095 | 19.347 | 19.624 | 19.988 |
| d(Å) | 4.677 | 4.644 | 4.584 | 4.519 | 4.438 |

## *Mechanical properties of polyimide films*

In order to elucidate the effect of OBBA/ODA copolymerization ratio on the mechanical properties of polyimide films, their tensile properties were further measured. As shown in Table 4, the symmetric structure improved the regularity of polymer molecular chains, which was conducive to the mechanical properties of films. The tensile strength, elastic modulus, and elongation at the break of the polyimide films varied in the ranges of 39.7–87.3 MPa,

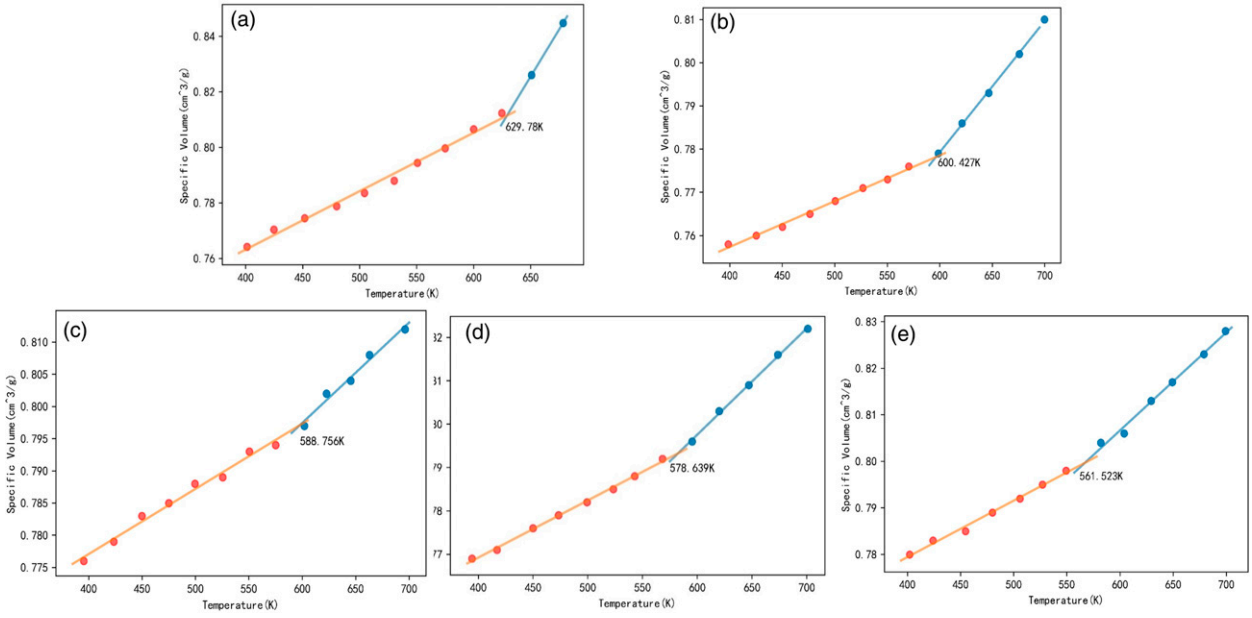


**Figure 5.** (a), (b), (c), (d) and (e) are the simulated calculation of glass transition temperature of OBBA/ODA copolymerization ratio of 0%, 1%, 5%, 10% and 20% respectively.

**Table 3.** Thermal and mechanical properties of polyimide films.

| Sample | $T_{d5\%}$ (°C) | $T_{d10\%}$ (°C) | $R_{W800}$ (°C) | $T_g$ (°C) | CTE(ppm/k) |
|---|---|---|---|---|---|
| PI-0 | 514 | 551 | 53.80 | 374 | 38.01 |
| PI-1 | 548 | 572 | 54.53 | 381 | 34.32 |
| PI-2 | 545 | 571 | 55.14 | 354 | 39.03 |
| PI-3 | 547 | 570 | 56.41 | 338 | 52.32 |
| PI-4 | 458 | 532 | 49.69 | 317 | 57.93 |

1.645–2.612 GPa, and 3.63%–15.62%, respectively. At the molecular level, the rigidity and flexibility of the molecular chain play an important role in its tensile parameters. For example, the introduction of a flexible chain can increase the elongation at break and toughness of the polymer structure. In turn, the rigid components exert a positive influence on the elastic modulus and tensile strength of the polymer. Therefore, the enhancement in tensile characteristics of the PI films with the increase of the OBBA/ODA ratio was attributed to the high quantity of benzene rings in OBBA. Each OBBA molecule contains two biphenyls, so the addition of aromatic structures will improve its tensile strength and elastic modulus. Meanwhile, the elongation at the break of the polyimide films was improved to a small extent only, mainly because of the high glass transition temperatures. It is worth mentioning that such films often undergo brittle fracture during the tensile test and even get broken before reaching the glass transition point regardless of their flexibility. On the other hand, a slight increase in the elongation at break at the low copolymerization ratio was owing to the fact that the contribution from flexible constituents was greater than that from biphenyl units.

## Simulation analysis

According to the free volume theory,[28–30] when the polymer is above the glass transition temperature, its volume expands upon heating, the chain segments thaw, and the range of activity noticeably increases. In this work, the density of polymers was studied at different temperatures, and the specific volume was then obtained as the reciprocal of the density and plotted as a function of temperature Figure 5. In the curves, the deflection points corresponded to the glass transition temperatures. Based on the fitting results, the glass transition temperatures of PI0-PI4 films ranged from 288.373 to 356.63°C with the increase of OBBA/ODA

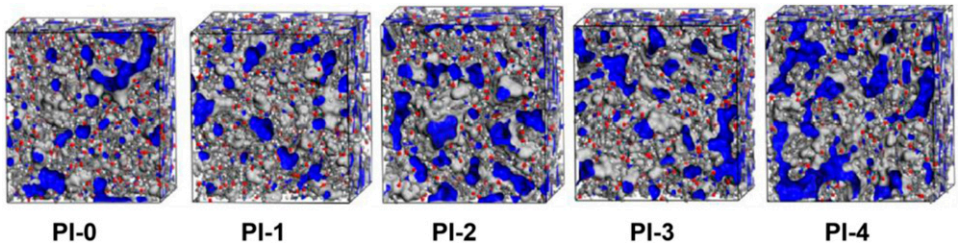


**Figure 6.** Molecular dynamic simulations of the molecular cells of the PIs.

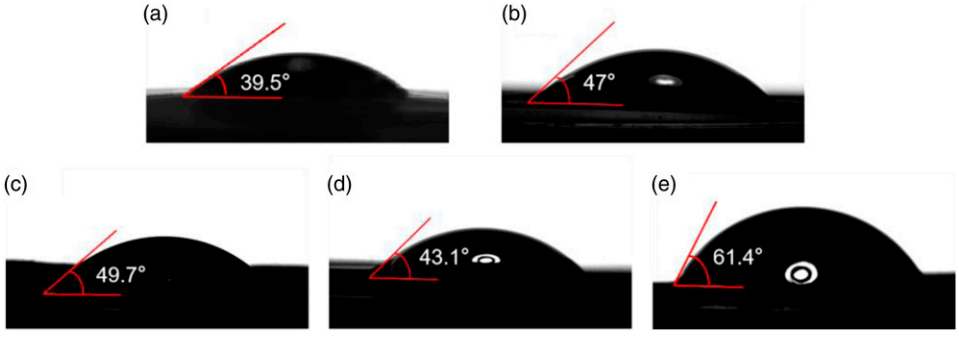


**Figure 7.** (a) (b) (c) (d) (e) is the contact angle test of polyimide film with OBBA/ODA copolymerization ratio of 0, 1%, 5%, 10% and 20% respectively.

**Table 4.** Mechanical properties of polyimide film.

| Sample | Tensile Strength (MPa) | Elastic Modulus (GPa) | Elongation at break (%) |
|---|---|---|---|
| PI-0 | 55.8 | 1.645 | 8.42 |
| PI-1 | 85.1 | 2.027 | 15.62 |
| PI-2 | 85.0 | 2.112 | 11.94 |
| PI-3 | 49.4 | 2.380 | 3.57 |
| PI-4 | 87.3 | 2.612 | 7.954 |

copolymerization ratio, showing a downward trend for PI-0-PI-4 specimens by analogy with the situation observed in. The gray-filled area in Figure 6 represents the volume occupied by the polymer, and the blue-filled area denotes the free volume. As seen from Figure 6 and Table 5, as the OBBA ratio increased, the free volume also became larger. Thus, it is proved that the introduction of fatty chains and ether bonds drastically increases the flexibility of the system, promoting fast defrosting and easier flow of each chain segment. In addition, biphenyls exert a strong effect on the free volume of the chains, and abundant benzene ring structures can play a supporting role in the system, providing more space for chain segment expansion.

**Table 5.** FFV of the PIs.

| Sample | Total volume | Free volume | FFV |
|---|---|---|---|
| PI-0 | 50,930.20 | 8884.77 | 0.174 |
| PI-1 | 47482.47 | 8771.09 | 0.185 |
| PI-2 | 50256.95 | 10942.8 | 0.218 |
| PI-3 | 50751.86 | 11335.51 | 0.223 |
| PI-4 | 53,057.19 | 12604.38 | 0.238 |

## *Hydrophilicity and hydrophobicity of polyimide films*

In order to evaluate the affinity of the polyimide films for water molecules and their hydrophobicity, contact angle

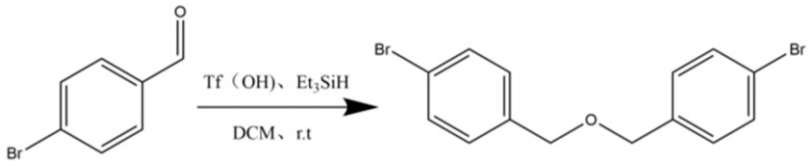


**Scheme 1.** Synthesis reaction formula of intermediate.

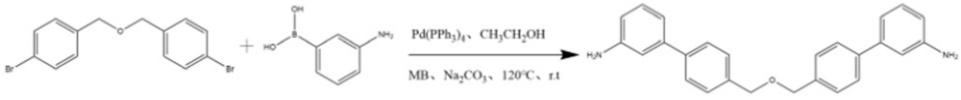


**Scheme 2.** Synthesis reaction formula of intermediate OBBA.

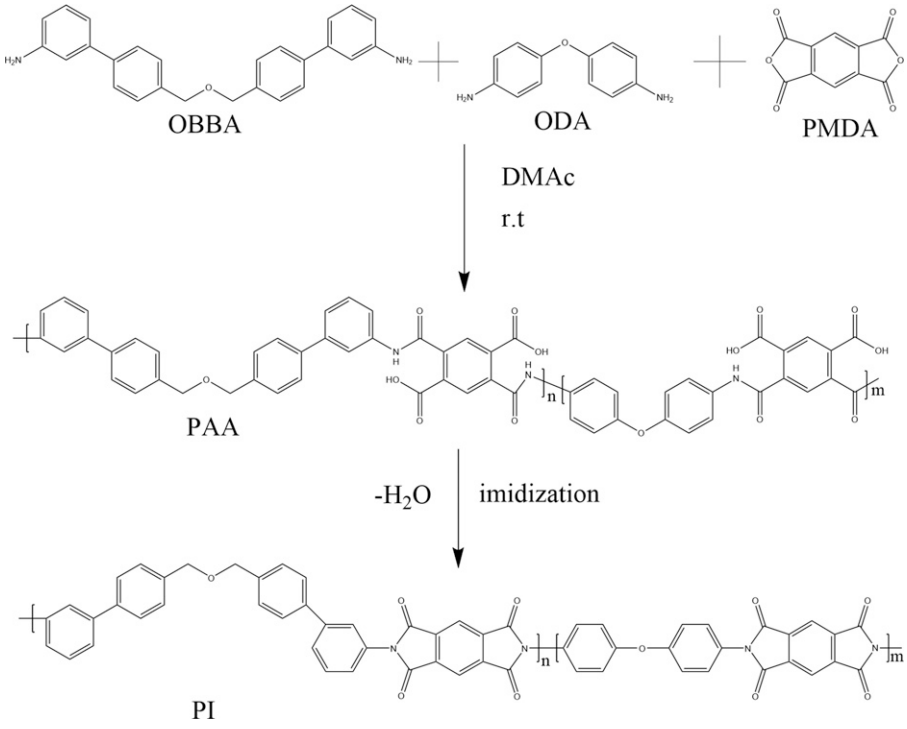


**Scheme 3.** Synthesis of flexible polyimide.

experiments were carried on. A water drop was applied to each film, and the contact angle between them was then measured using the optical microscope. The experimental results are shown in Figure 7. It is not difficult to see that the contact angle of OBBA increased with the copolymerization ratio, which was due to the hydrophobic fatty chains present in OBBA. In turn, the effect of the hydrophilic ether bonds as part of ODA on the wetting properties of the entire system was insignificant. Scheme 1–3.

## Conclusions

A flexible diamine containing ether bonds and fatty chains was successfully produced through the Suzuki reaction. Copolymerization of diamine and ODA/PMDA taken in different proportions enabled one to obtain a series of polyimide films. Compared with a pure ODA/PMDA system, the chain and interchain forces in the copolymerized films were enhanced to a large extent, promoting a close and orderly stacking of the molecular chains, which effectively reduced the glass transition temperature and improved the thermodynamic and mechanical properties of the films. The increase in the copolymerization ratio from 1 to 10% made the glass transition temperature decreased by 15% (from 374°C to 317°C). In turn, the tensile strength and elastic modulus increased from 55.8 to 87.3 MPa and from 1.645 to 2.612, respectively. Therefore, the introduction of the rigid biphenyl along with flexible ether bonds and aliphatic linkages into the diamine structure is a promising way to achieve a balance between the low glass transition temperature and high mechanical properties without seriously damaging the thermal characteristics of the polymer.

### Acknowledgments

In this section, you can acknowledge any support given which is not covered by the author contribution or funding sections. This may include administrative and technical support, or donations in kind (e.g., materials used for experiments).

### Author contributions

Jinshui Lu: Conceptualization, Methodology, Investigation. Weipeng Chen: Investigation, Data curation. Heng Liu: Formal analysis. Jiangrong Luo: Investigation. Jinyuan Zhang: Investigation. Ziqing Wang: Investigation. Yidong Liu: Writing – review & editing. Yonggang Min: Writing – review & editing, Supervision, Funding acquisition.

### Declaration of conflicting interests

The author(s) declared no potential conflicts of interest with respect to the research, authorship, and/or publication of this article.

### Funding

The author(s) disclosed receipt of the following financial support for the research, authorship, and/or publication of this article: This work was supported by the authors gratefully acknowledge the National Key R&D Program of China (No. 2020YFB0408100), Guangdong Innovative and Entrepreneurial Research Team Program (No. 2016ZT06C412), National Natural Science Foundation of China (NSFC; No. U20A20340).

### ORCID iD

Yonggang Min https://orcid.org/0000-0002-2804-9346

### References

1. Lin B and Xu X. Preparation and properties of cyano-containing polyimide films based on 2,6-Bis(4-aminophenoxy)- benzonitrile. *Polym Bull* 2007; **59**: 243–250.
2. Nicholls AR, Perez Y, Pellisier M, et al. Thermomechanical characterization of thermoplastic polyimides to improve the chain collaboration via ureidopyrimidone endcaps. *Polym Eng Sci* 2019; **59**: 2231–2246.
3. Jiao Y, Chen G, Zhou H, et al. Synthesis and properties of processable poly(benzimidazole-imide)s based on 2-(3-aminophenyl)-5-aminobenzimidazole. *J Polym Res* 2019; **26**.
4. Tan W-Y, Jian L-F, Chen W-P, et al. A facile strategy for intrinsic low-dk and low-df polyimides enabled by spirobifluorene groups. *Chin J Polym Sci* 2022; **209**: 1–9.
5. Luo JR, Liu YD, Liu H, et al. Synthesis and characterization of polyimides with naphthalene ring structure introduced in the main chain. *.Materials* **15**, 2022.
6. Kausar A, Sher F, Hazafa A, et al. Biocomposite of sodium-alginate with acidified clay for wastewater treatment: Kinetic, equilibrium and thermodynamic studies. *Int J Biol Macromol* 2020; **161**: 1272–1285.
7. Rasheed T, Hassan AA, Kausar F, et al. Carbon nanotubes assisted analytical detection e Sensing/delivery cues for environmental and biomedical monitoring. *TrAC, Trends Anal Chem* 2020; **132**: 116066.
8. Bao F, Dai X, Dong Z, et al. Fabrication and properties of polyimide copolymer fibers containing pyrimidine and amide units. *J Mater Sci* 2020; **55**: 11763–11778.
9. Rohaizad A, Shahabuddin S, Shahid MM, et al. Green synthesis of silver nanoparticles from Catharanthus roseus dried bark extract deposited on graphene oxide for effective adsorption of methylene blue dye. *J Environ Chem Eng* 2020; **8**.
10. Cunha MR, Lima EC, Lima DR, et al. Removal of captopril pharmaceutical from synthetic pharmaceutical-industry wastewaters: Use of activated carbon derived from Butia catarinensi. *J Environ Chem Eng* 2020; **8**.
11. Rasheed T, Shafi S, Bilal M, et al. Surfactants-based remediation as an effective approach for removal of environmental pollutants—A review. *J Mol Liq* 2020; **318**: 113960.
12. Altaf F, Niazi MBK, Jahan Z, et al. Synthesis and characterization of PVA/starch hydrogel membranes incorporating

essential oils aimed to be used in wound dressing applications. *J Polym Environ* 2021; **29**: 156–174.
13. Sehar S, Sher F, Zhang S, et al. Thermodynamic and kinetic study of synthesised graphene oxide-CuO nanocomposites: A way forward to fuel additive and photocatalytic potentials. *J Mol Liq* 2020; **313**: 113494.
14. Lian M, Lu X and Lu Q. Synthesis of superheat-resistant polyimides with high Tg and low coefficient of thermal expansion by introduction of strong intermolecular interaction. *Macromolecules* 2018; **51**: 10127–10135.
15. Nazarychev VM, Lyulin AV, Larin SV, et al. Molecular dynamics simulations of uniaxial deformation of thermoplastic polyimides. *Soft Matter* 2016; **12**: 3972–3981.
16. Yen H-J, Wu J-H, Huang Y-H, et al. Novel thermally stable and soluble triarylamine functionalized polyimides for gas separation. *Polym Chem* 2014; **5**.
17. Behniafar H and Abedini-pozveh A. Flexible, low-colored and transparent thin films prepared from new thermo-stable and organo-soluble poly(amide-imide)s. *Polym Degrad Stabil* 2011; **96**: 1327–1332.
18. Comesaña-Gándara B, Calle M, Jo HJ, et al. Thermally rearranged polybenzoxazoles membranes with biphenyl moieties: Monomer isomeric effect. *J Membr Sci* 2014; **450**: 369–379.
19. Kim SD, Lee S, Heo J, et al. Soluble polyimides with trifluoromethyl pendent groups. *Polymer* 2013; **54**: 5648–5654.
20. Liaw D-J and Chen W-H. High glass transitions of novel organosoluble polyamide-imides based on noncoplanar and rigid diimide-dicarboxylic acid. *Polym Degrad Stabil* 2006; **91**: 1731–1739.
21. Lin CH, Chang SL, Peng LA, et al. Organo-soluble phosphinated polyimides from asymmetric diamines. *Polymer* 2010; **51**: 3899–3906.
22. Liu C, Wang J, Lin E, et al. Synthesis and properties of phthalonitrile-terminated oligomeric poly(ether imide)s containing phthalazinone moiety. *Polym Degrad Stabil* 2012; **97**: 460–468.
23. Liu J, Zhang Q, Xia Q, et al. Synthesis, characterization and properties of polyimides derived from a symmetrical diamine containing bis-benzimidazole rings. *Polym Degrad Stabil* 2012; **97**: 987–994.
24. Shockravi A, Abouzari-Lotf E, Javadi A, et al. Preparation and properties of new ortho-linked polyamide-imides bearing ether, sulfur, and trifluoromethyl linkages. *Eur Polym J* 2009; **45**: 1599–1606.
25. Yang F, Li Y, Bu Q, et al. Characterizations and thermal stability of soluble polyimide derived from novel unsymmetrical diamine monomers. *Polym Degrad Stabil* 2010; **95**: 1950–1958.
26. Barikani M and Mehdipour-Ataei S. Synthesis, characterization, and thermal properties of novel arylene sulfone ether polyimides and polyamides. *J Polym Sci Polym Chem* 2000; **38**: 1487–1492.
27. Vrentas and Duda JL Diffusion in polymer-solvent systems. I. reexamination of the free-volume theory. *J Polym Sci Polym Phys Ed*, (1977), **15**(3), 403-416.
28. Zielinski JM and Duda JL. Predicting polymer/solvent diffusion coefficients using free-volume theory. *AIChE J* 1992; **38**: 405–415.
29. Hong S-U. Prediction of polymer/solvent diffusion behavior using free-volume theory. *Ind Eng Chem Res* 1995; **34**: 2536–2544.
30. Dlubek G, Saarinen K and Fretwell HM. The temperature dependence of the local free volume in polyethylene and polytetrafluoroethylene: a positron lifetime study. *J Polym Sci B Polym Phys* 1998; **36**(9): 1513–1528.